Intrinsic correlation between the fraction of liquid-like zones and the β-relaxation in high-entropy metallic glasses

Y. J. Duan[a,b], L.T. Zhang[a], J. C. Qiao[a,*] , Y.J. Wang[c,d], Y. Yang[e,f], T. Wada[g], H. Kato[g], J.M. Pelletier[h], E. Pineda[b,*], D. Crespo[b]

[a]*School of Mechanics, Civil Engineering and Architecture, Northwestern Polytechnical University, Xi'an 710072, China*

[b]*Department of Physics, Institute of Energy Technologies, Universitat Politècnica de Catalunya, Barcelona 08019, Spain*

[c]*State Key Laboratory of Nonlinear Mechanics, Institute of Mechanics, Chinese Academy of Sciences, Beijing 100190, China*

[d]*School of Engineering Science, University of Chinese Academy of Sciences, Beijing 100049, China*

[e]*Department of Mechanical Engineering, College of Engineering, City University of Hong Kong, Tat Chee Avenue, Kowloon Tong, Kowloon, Hong Kong SAR, China*

[f]*Department of Materials Science and Engineering, College of Engineering, City University of Hong Kong, Tat Chee Avenue, Kowloon Tong, Kowloon, Hong Kong SAR, China*

[g]*Institute for Materials Research, Tohoku University, Sendai 980-8577, Japan*

[h]*Université de Lyon, MATEIS, UMR CNRS5510, Bat. B. Pascal, INSA-Lyon, F-69621 Villeurbanne Cedex, France*

Submitted to *Physical Review Letters*

(Version: August 27, 2022)

*Corresponding author.

Prof. Dr. J.C. Qiao, E-mail address: qjczy@nwpu.edu.cn

Prof. Dr. E. Pineda, E-mail address: eloi.pineda@upc.edu

Abstract

Lacking the structural information of crystalline solids, the origin of the relaxation dynamics of metallic glasses is unclear. Here we report the evolution of stress relaxation of high-entropy metallic glasses with distinct β-relaxation behavior. The fraction of liquid-like zones, determined at each temperature by the intensity of stress decay, is shown to be directly related to both the aging process and the spectrum of relaxation modes obtained by mechanical spectroscopy. The results shed new light on the intrinsic correlation between the static and dynamic mechanical response in high-entropy and conventional metallic glasses, pointing towards a sluggish diffusion high-entropy effect in the liquid dynamics.

Letter

Owing to the disordered atomic structure, metallic glasses (MGs) show unique properties [1-4]. Besides, high-entropy alloys (HEAs), containing equimolar concentrations of each component, have been developed recently [5-7]. Benefitting from the high configurational entropy, large lattice distortion, sluggish diffusion and the cocktail effect [8,9], HEAs exhibit distinctive physical and mechanical properties [5,9,10]. With the aim of blending the properties of MGs and HEAs, high-entropy metallic glasses (HEMGs) have been developed [11-13]. However, the existence of specific properties of HEMGs as compared to other families of MGs, especially the presence of a high entropy - sluggish diffusion effect [14] and its effects on the glass-to-liquid transition and the aging/rejuvenation processes, which are essential to control the glassy configuration and adjust the materials properties [11,15], have not been clearly demonstrated.

Dynamic mechanical analysis (DMA) [2], i.e. mechanical spectroscopy, and stress relaxation [16,17] have been proven powerful tools to characterize the dynamics of MGs [17,18]. Stress relaxation has been investigated at different length scales by experiments [16,19] and simulations [20]. Besides, secondary β-relaxation, preceding in temperature the collective, large-scale α-relaxation, is observed by mechanical spectroscopy and has been associated with local (nano-scale) atomic phenomena [20,21]. Although stress relaxation and mechanical spectroscopy observations are, respectively, the time and frequency domain responses of the same mechanical relaxation phenomenon, a direct evidence of the intrinsic correlation between β-relaxation and stress relaxation in MGs is still missing.

In this letter, we present a study over six different metallic glass formers. Three HEMGs and three 'conventional' MGs which are representative of the main compositional families of glass-forming alloys. By calorimetric and mechanical tests, we try to step forward in the solving of important questions, namely: What is the relation between the thermal activation of liquid like zones and the relaxation spectrum of metallic glasses? How the dynamical heterogeneity evolves during changes of the

glass state? And, finally, are there systematic dynamical differences between high-entropy and conventional metallic glass-formers?

For this purpose, we investigated the stress relaxation behavior of HEMGs and MGs following the stress decay under a constant strain while heating in isothermal steps. The stress decay was monitored for 1800 s in each step from room temperature to the glass transition. It is known that both stress and temperature are equally critical in controlling the stress relaxation dynamics of MGs [22-24], as the external stress reduces the apparent flow activation energy [24]. Here, the applied strains are small and equal from room temperature to the glass transition, always within 0.3-0.6%. Within this range the observed behaviors are basically produced by the temperature effects. The selected compositions for this study are three representative HEMGs, $La_{20}Ce_{20}Y_{20}Ni_{20}Al_{20}$ (La-HEMG), $Pd_{20}Pt_{20}Cu_{20}Ni_{20}P_{20}$ (Pd-HEMG) [25] and $Ti_{16.7}Zr_{16.7}Hf_{16.7}Cu_{16.7}Ni_{16.7}Be_{16.7}$ (Zr-HEMG) and three representatives of 'conventional' MGs, $La_{60}Ni_{15}Al_{25}$ (La-MG), $Pd_{40}Ni_{40}P_{20}$ (Pd-MG), and $Zr_{45}Cu_{50}Al_5$ (Zr-MG), with obvious different β-relaxation behaviors. As seen in the methods section in supplementary materials (**Figs. S1 (a,b)**), all these MGs have a significant supercooled liquid (SCL) region and excellent stability against crystallization. For each composition the tests were performed in both as-quenched samples (cooled from the melt at ~10^5-10^6 K s^{-1}) and relaxed samples (cooled from the SCL at 1.67×10^{-3} K s^{-1}).

The temperature dependence of the normalized loss modulus $\frac{E''}{E''_{\max}}$ obtained by DMA is shown in **Figs. 1 (a,b)**. With a driving frequency of 2 Hz, the maximum of loss modulus $E''_{\max}$, which corresponds to the α-relaxation peak, is observed at T_α= 504, 588 and 708 K for La-HEMG, Pd-HEMG and Zr-HEMG and at 488, 602 and 730 K for the La-MG, Pd-MG and Zr-MG, respectively. The β-relaxation is observed as a distinct peak [18,26] for the La-based glasses, a shoulder [17,18] for the Pd-based and an excess wing [27,28], almost merged into the α-relaxation, for the two glasses of the Zr family.

While crystalline defects and grain boundaries are crucial for the internal friction of crystalline metals [29], the heterogeneous nanoscale structure seems to be the main

factor in the case of MGs [30,31]. It has been accepted that MGs can be regarded as viscous, weak-bond regions caged in an elastic, strong-bond matrix, as described by the models based on flow units [32-34] or soft spots [33]. Within this picture, the β-relaxation is seen as a reversible process of local atomic rearrangement of these soft spots and it is closely correlated to the mechanical properties of glasses, particularly with the underlying mechanisms of plastic deformation [17,18].

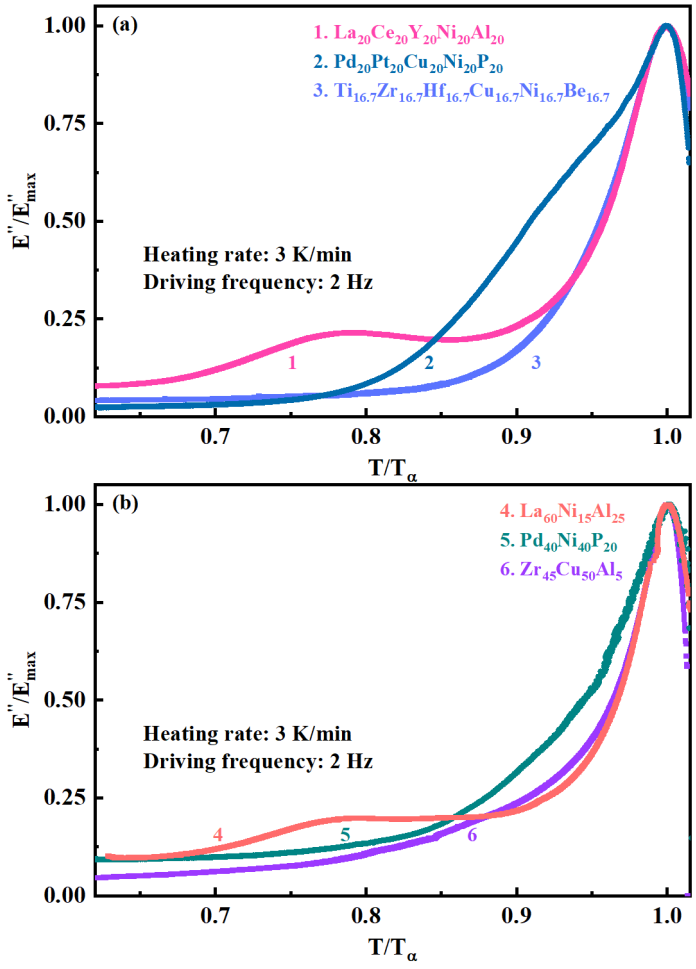

Figure 1. Normalized loss modulus $\frac{E''}{E''_{\max}}$ as a function of the normalized temperature T/T_α. T_α stands for the peak temperatures of α relaxation probed at 2 Hz. (a) HEMGs (b) 'conventional' MGs.

The stress drop of the HEMGs from room temperature to near T_α (for details see the methods section in supplementary materials) is shown in **Fig. 2 (a)-(c)**. After applying a constant strain, the stress relaxes with time. We define $\delta = \frac{\sigma_0 - \sigma_r}{\sigma_0}$ as the

intensity of stress relaxation, where σ_0 and σ_r are the initial and terminal stresses of each 30 min relaxation curve. The intensity of stress drop δ can be associated to the fraction of liquid-like activated flow units and to viscosity [19,35]. The σ_0 and σ_r of each relaxation curve are depicted as open circles and squares, respectively. One can notice that the decay of σ_0 is not prominent until close to T_g, whereas the decay of σ_r accelerates near T_β (the temperature of the β-relaxation) and then drops to zero near T_g. In order to more clearly reveal the influence of the distinct β-relaxation behaviors, in **Figs. 2 (d)-(f)** we depict together the evolution of δ (for 30 min of stress relaxation each 3 K step) and the normalized loss modulus $\frac{E''}{E''_{\max}}$ (driving frequency of 2 Hz and a heating rate of 3 K min^{-1}). With the increase of temperature near T_β, both of these magnitudes accelerate their rising reaching a maximum around T_g. The evolution of δ in the different HEMGs exhibits a hint of a peak for the La-HEMG a shoulder for Pd-HEMG and an excess wing for Zr-HEMG, replicating the β-relaxations.

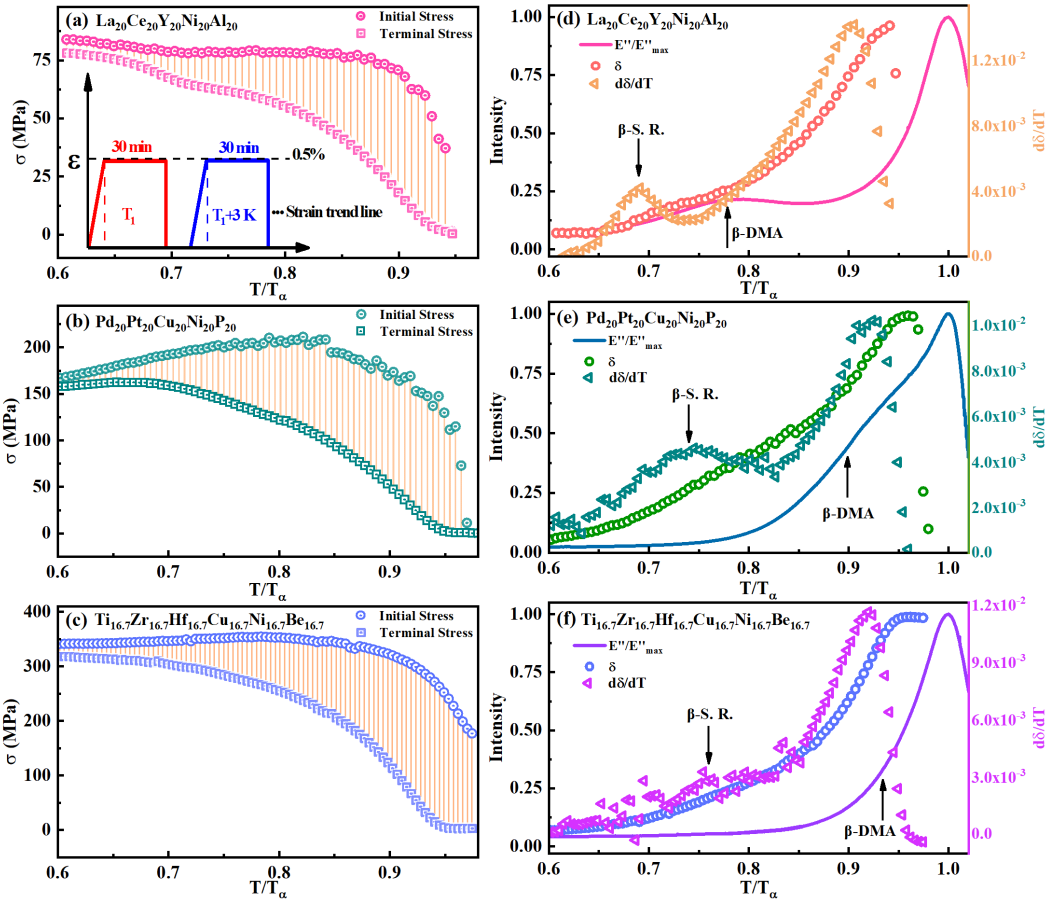

Figure 2. Stress relaxation measured at stepping temperature from room temperature to T_α for

(a) La-HEMG, (b) Pd-HEMG, and (c) Zr-HEMG. Evolution with temperature of stress drop δ, stress drop change rate $\frac{d\delta}{dT}$ and normalized loss modulus $\frac{E''}{E''_{\max}}$ of (d) La-HEMG, (e) Pd-HEMG, and (f) Zr-HEMG.

Interpreting δ as the fraction of liquid-like activated flow units [19][48], the increase of δ indicates that a higher fraction of atoms are unfrozen to undergo inelastic deformation [36,37]. This fact can be viewed as the increase of atomic/molecular mobility caused by the thermal activation of microscopic movements. It is interesting to discuss the similarity between the loss modulus and the intensity of stress relaxation. $\delta(T)$ shows the same features as $\frac{E''(T)}{E''_{\max}}$, but shifted to lower temperatures. In this work, the driving frequency of DMA experiments was 2 Hz, while the "effective driving frequency" of the stress relaxation tests can be estimated as $f \sim \frac{1}{30\ \text{min}} = 6\times10^{-4}$ Hz. It is well known that that the loss modulus is shifted to low temperatures as frequency decreases [38]. Following ref. [19], $\delta(T)$ can be interpreted as the fraction of liquid-like zones, i.e. zones that can relax stress within the duration of the test. Similarly, the integration of the relaxation spectrum obtained by DMA, $\int_0^T \frac{E''(T)}{E''_{\max}} dT$, is proportional to the fraction of relaxation modes faster than $\sim f^{-1}$. Therefore, the derivative $d\delta(T)/dT$ should be proportional to $E''(T)/E''_{\max}$ at a frequency of $f \sim 6\times10^{-4}$ Hz. **Figs. 2 (d)-(f)** shows the behavior of $d\delta(T)/dT$ with clear α and β peaks displaced to lower temperatures, as expected for such a low driving frequency. For all the three materials, the position of the $d\delta(T)/dT$ maximum is found at $\sim 0.9T_{\alpha,2\text{Hz}}$, in agreement with the temperatures at which the slope of the $\tau_c(T)$ (see **Fig 3** and discussion below) is observed to change, indicating the onset of the dynamic glass transition for this frequency. For Pd-HEMG, the α and β become well separated in comparison with the 'shoulder' observed at $f = 2$ Hz. For Zr-HEMG, the excess wing observed at $f = 2$ Hz is moved towards lower temperatures and starts to be similar to a broad shoulder of low intensity. The same intrinsic correlation between loss modulus and $d\delta(T)/dT$ can be found in the three 'conventional' La, Pd and Zr MGs (see **Figs.**

156 **S2** of supplementary materials). This direct relationship between the fraction of liquid-
157 like zones and the spectrum of relaxation modes is in agreement with the view of MGs
158 being composed by a spatial distribution of zones of different relaxation time [39] or,
159 in other words, more or less liquid-like in nature. The transition from inhomogeneous
160 to homogenous flow is associated to the fraction of liquid-like zones reaching a
161 percolation or threshold fraction of around 25% [19]. Therefore, the results presented
162 here suggest that one could establish a readily way of estimating the inhomogeneous to
163 homogeneous line in a strain rate – temperature map by integrating the $\frac{E''(T)}{E''_{\max}}$ spectra
164 obtained at different frequencies.

165 The results in **Figs. 2** correspond to as-quenched samples. In this samples, the
166 evolution of liquid-fraction zones is not only due to the activation of the β and α
167 relaxations as temperature increases, but also to the physical aging process (or structural
168 relaxation) occurring during the tests [40]. Physical aging drives the glass to more stable
169 and denser configurations, reducing the excess free volume in the structure and so also
170 reducing the intensity of the secondary relaxation and the fraction of liquid-like zones.
171 **Figs. S3** in supplementary materials show the results of DMA and stress relaxation tests
172 on relaxed samples. The secondary peak in $E''(T)/E''_{\max}$ shows a reduced intensity as
173 expected for well relaxed materials, as now reflects the activation of the β relaxation in
174 a structure with comparatively much less liquid-like zones. For $d\delta(T)/dT$ the peak is
175 clearly reduced, but still evident, for the Pd glasses while it becomes almost
176 indistinguishable for the La systems. The same effect is observed in calorimetry (see
177 **Figs. S4**) where the activation of the β relaxation shows a clear signature in Pd systems
178 while it is negligible in La based. This suggests a different nature of the secondary
179 relaxation in Pd and La systems. It can be correlated to the increase of the liquid-like
180 volume fraction in Pd, whereas in La systems it seems to be related to an isolated
181 mobility mechanism which remains too fast to contribute to the overall stress relaxation
182 at longer times.

183 In order to further characterize the relaxation behavior of the glasses, the stress
184 relaxation curves at each temperature step were fitted to the phenomenological

Kohlrausch-Williams-Watts (KWW) equation [19,41]

$$\sigma(t) = \sigma_0 \exp\left(-\frac{t}{\tau_c}\right)^{\beta_{\mathrm{KWW}}} \quad (1)$$

where $\sigma(t)$ is the stress at time t, β_{KWW} is a stretching exponent, a parameter linked to the dynamic heterogeneity, and τ_c is the stress relaxation timescale. Some selected results are shown in **Fig. 3**. **Figs. S5-S7** in supplementary materials show the relaxation curves at various temperatures and details of the corresponding fittings with **Eq. (1)**. **Figs. S8**, show the results for the La, Pd and Zr-MGs. The overall behavior is similar for all the alloys. At $T/T_\alpha < 0.7$ the stress relaxation achieved during 30 min is small, less than 15%. This indicates that the relaxation timescale is much longer than the experimental time window. For the relaxed samples, this happens until $T/T_\alpha \lesssim 0.85$ due to the reduction of liquid-like zones in the more densified state. The results in this low temperature range are not shown in **Fig. 3** and will not be discussed here as a longer experimental relaxation step would be necessary to proper characterize τ_c and β_{KWW}. In the temperature region $0.7 < T/T_\alpha < 0.9$, $\tau_c(T)$ decreases with temperature, going from values above 10^4 s towards a value of $\tau_c \sim 10^3$ s at $T/T_\alpha \sim 0.9$. The parameter β_{KWW} varies within 0.35 to 0.6, which are typical values in the relaxation of amorphous alloys [19,26,42,43].

The physical aging of the glasses during the tests seems reflected on the behavior of $\beta_{\mathrm{KWW}}(T)$. Although aging drives the system to a lower energy state with less overall internal friction [38], various recent studies have shown that the underlying relaxation time distribution becomes more heterogeneous during aging [16,43-45]. Thus, although the total intensity of stress relaxation is smaller in the aged samples, the different timescales participating in it become more separated as indicated by a decrease of $\beta_{\mathrm{KWW}}(T)$. This phenomenon is also observed here in the temperature range going from T/T_α=0.7 to 0.8. The as-quenched samples start with a $\beta_{\mathrm{KWW}}(T) \sim 0.5$, a level of dynamical heterogeneity similar to what is observed in the SCL [46]. As soon as the fraction of activated liquid-like zones increases, the aging process is allowed to proceed, and $\beta_{\mathrm{KWW}}(T)$ decreases until values around 0.3, as it was also observed for very well aged glassy states in other works [16,43,44]. At the higher temperatures, the transition

from a relaxed glass towards the liquid state shows, in parallel, the increase of the fraction of liquid-like-zones and the $\beta_{\mathrm{KWW}}(T)$ parameter, which returns to values in the range 0.5-0.6 at the glass transition. The reason of the more constant behavior of $\beta_{\mathrm{KWW}}(T)$ in the La-HEMG and MG (see **Fig. S3**) is not clear but may be related to the presence of a distinct secondary process that dominates the atomic mobility at the temperature range T/T_{α}=0.7 - 0.8. It is worth noticing that the evolution of $\beta_{\mathrm{KWW}}(T)$ (shown in **Figs. 3b and 3c**) seems to be concave regardless of the material state. The pre-annealed and well-relaxed samples show also a striking concave nature (see **Fig. S9**). However, the duration of the isothermal steps of the experiments presented in this work is not long enough to conclusively study the behavior of relaxed samples at low temperatures.

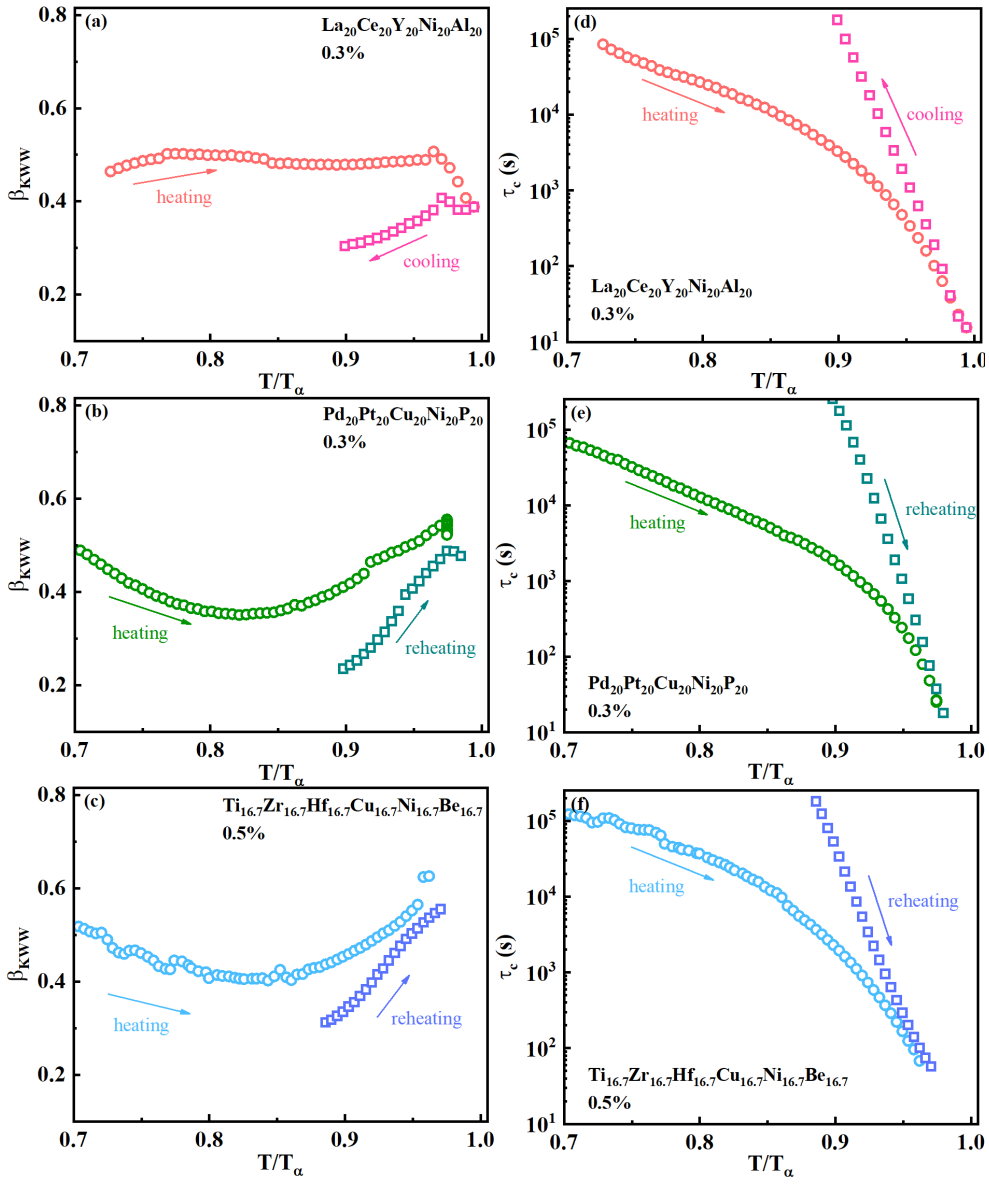

Figure 3. The fitted KWW parameters β_{KWW} of (a) La-HEMG, (b) Pd-HEMG and (c) Zr-HEMG and τ_c (d) La-HEMG, (e) Pd-HEMG and (f) Zr-HEMG with initial as-quenched state and with well relaxed state (second cycle of stress relaxation measurements after slowly cooling from T_g).

At $T/T_\alpha \sim$ 0.9, the relaxation times of the six glasses are of the same timescale than the isothermal steps (2100 s), this allows the glasses to get closer to an ergodic state within each temperature step. This is observed by the progressive change of the slope of $\tau_c(T)$, which signals the transition from glass to SCL dynamics. Accordingly, between $0.9 < T/T_\alpha < 0.95$ the relaxation dynamics are more accelerated by the increase of temperature. At $T/T_\alpha \sim$0.93-0.94, all materials achieve full relaxation

during the 30 min tests. Finally, above this temperature, the onset of crystallization is clearly detected in the shape of the relaxation curves, thus also dictating the upper limit of the validity of the KWW equation to describe the experimental data (see **Figs. S5-S7**).

Finally, we will discuss the intrinsic effect of high entropy in the glass and liquid dynamics. The difference of specific heat between the glassy alloys and the crystalline baselines was measured by differential scanning calorimetry (DSC). The $c_p(T)$ curves are given in **Figs. S4** in supplementary materials. **Fig. 4 (a)-(c) and (g)** shows the step $\Delta c_{p,T_g} = c_{p,l} - c_{p,g}$ at the glass transition and the integration $\Delta S_{lg-x} = \int_{T_1}^{T_2} \frac{c_{p,lg}(T) - c_{p,x}(T)}{T} dT$, which corresponds to the excess of entropy between the amorphous (glass/liquid) and the crystallized samples. It can be observed that the HEMGs systematically show higher glass transition steps, $\Delta c_{p,T_g}$, and configurational entropies in comparison with the conventional MGs.

The mobility in the glass is determined by both the aging process and the fast part of the relaxation spectrum, dominated by the β-relaxation and the high-frequency wing of the α-process. The specific shape of this spectrum is primarily dependent on the kind of metallic glass family, independently of the high-entropy or 'conventional' nature of the alloys. Interestingly, the value $E_\beta/RT_g \approx 25 \pm 2$ (see **Table S1**) derived from stress relaxation is consistent with the empirical relationship $E_\beta/RT_g \approx 26$ found in various MGs [17,18], in agreement with previous dynamic mechanical analyses [47] and amplitude-modulation atomic force microscopy results [48]. On the other hand, the relaxation tests performed in this work, allows us to study the temperature evolution of the dynamics in the region of the glass transition, dominated by the α (or viscous) relaxation. **Fig. 4 (d)-(f)** shows the evolution with temperature of τ_c in the region where it becomes shorter than 300 s. The fragility of the liquid, $m = \frac{d(\log \tau_c)}{d(T_g/T)}$, or equivalently, the apparent activation energy of the relaxation, E_α, can be calculated in this region. It is found that the HEMGs show always a stronger liquid behavior than

their MGs counterparts. At the same relative temperatures respect to the glass transition, the Pd and La HEMGs show slower dynamics that their corresponding 'conventional' counterparts.

Configurational and vibrational entropy contribute to the total entropy of metallic glasses [49-51]. The vibrational entropy in MGs (and their undercooled liquids) is approximately equal to that of the corresponding crystals, [49,52], and this implies that the excess entropy of MGs can be mainly attributed to the configurational entropy difference [50,52]. The rough correlation usually observed in glass formers between the Δc_p step at the glass transition and the liquid fragility is not fulfilled for the studied alloys and this can be another trait related to the high-entropy effect. The larger Δc_p of the HEMGs indicates that, in these alloys, the glass to liquid transition unfrozens the possibility to explore a larger quantity of configurations [53]. However, this is not correlated to faster dynamics (or a more fragile liquid behavior) but to the high entropy of mixing of these compositions. This points towards the sluggish diffusion high-entropy effect in the liquid dynamics as suggested in other works [14,54,55].

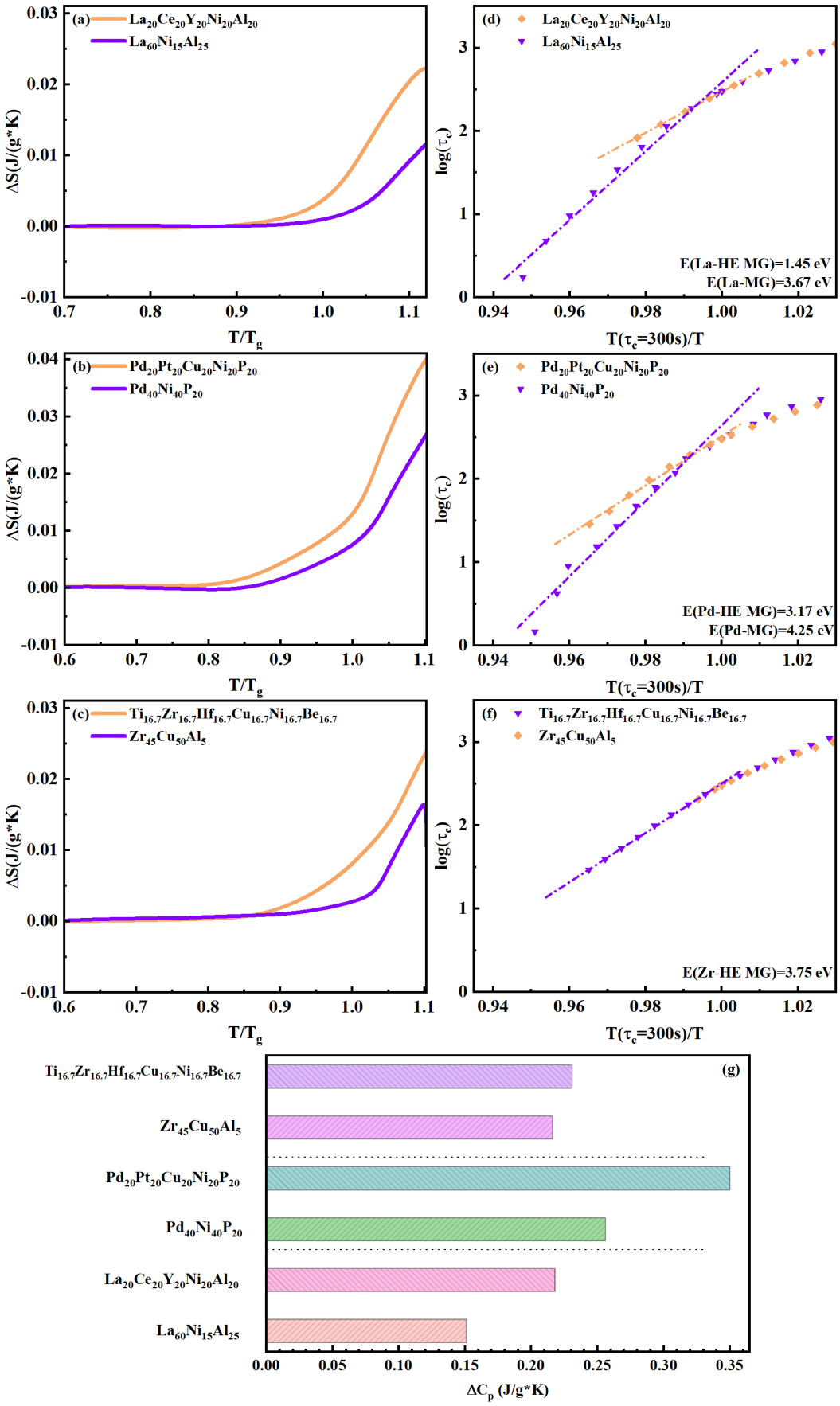

Figure 4. The excess of entropy ΔS of (a) La-based, (b) Pd-based and (c) Zr-based HEMGs

and MGs. Stress relaxation time τ_c vs reciprocal temperature $T(\tau_c = 300s)/T$ and fitted Arrhenius plots for (d) La-based, (e) Pd-based and (f) Zr-based HEMGs and MGs. (g) The step Δc_p at the glass transition of well relaxed samples of HEMGs and MGs.

In summary, the evolution of stress relaxation of high entropy and conventional MGs with different types of β-processes was investigated. The study of the timescale and shape of the relaxation curves indicates that HE-MGs tend to have an enhanced strong liquid behavior above the dynamic glass transition, and that aging of the glass increases the relative separation of the relaxation times contributing to the stress relaxation, as reflected in the decrease of the β_{KWW} exponent. Importantly, this work shows that the fraction of zones that behave liquid-like during a fixed time interval is proportional to the relaxation mode spectrum at the corresponding low frequency. Our results shed new light on the intrinsic correlation between the static and dynamic mechanical response in high-entropy and conventional metallic glasses, and they provide a practical guideline for understanding, and subsequently controlling, the mechanical behavior of HE-MGs.

This work is supported by the NSFC (Grant No. 51971178), the Fundamental Research Funds for the Central Universities (Grant No. D5000220034), the Natural Science Basic Research Plan for Distinguished Young Scholars in Shaanxi Province (Grant No. 2021JC-12). E. Pineda and D. Crespo acknowledge financial support from the research project PID2020-112975GB-I00 funded by MCIN/AEI /10.13039/501100011033 and from Generalitat de Catalunya (AGAUR grant 2017SGR0042). Y.J. Wang was financially supported by NSFC (Grant No. 12072344) and the Youth Innovation Promotion Association of the Chinese Academy of Sciences. Y. Yang acknowledges financial support from Research Grant Council (RGC), the Hong Kong government through the General Research Fund (GRF) with the grant numbers CityU11200719 and CityU11213118. Y. J. Duan is sponsored by the Innovation Foundation for Doctor Dissertation of Northwestern Polytechnical University (No.

CX202031) and China Scholarship Council (CSC) under Grant 202006290092.

References

[1] J. Schroers and W. L. Johnson, Phys. Rev. Lett. **93**, 255506 (2004).

[2] W. H. Wang, Prog. Mater Sci. **106**, 100561 (2019).

[3] M. R. Chellali, S. H. Nandam, and H. Hahn, Phys. Rev. Lett. **125**, 205501 (2020).

[4] A. D. Phan, A. Zaccone, V. D. Lam, and K. Wakabayashi, Phys. Rev. Lett. **126**, 025502 (2021).

[5] D. B. Miracle, Nat. Commun. **10**, 1805 (2019).

[6] S. Wei, S. J. Kim, J. Kang, Y. Zhang, Y. Zhang, T. Furuhara, E. S. Park, and C. C. Tasan, Nat. Mater. **19**, 1175 (2020).

[7] X. Chang, M. Zeng, K. Liu, and L. Fu, Adv. Mater. **32**, 1907226 (2020).

[8] D. B. Miracle and O. N. Senkov, Acta. Mater. **122**, 448 (2017).

[9] E. P. George, D. Raabe, and R. O. Ritchie, Nat. Rev. Mater. **4**, 515 (2019).

[10] P. Koželj, S. Vrtnik, A. Jelen, S. Jazbec, Z. Jagličić, S. Maiti, M. Feuerbacher, W. Steurer, and J. Dolinšek, Phys. Rev. Lett. **113**, 107001 (2014).

[11] W. H. Wang, JOM **66**, 2067 (2014).

[12] E. Goncharova, R. Konchakov, A. Makarov, N. Kobelev, and V. Khonik, J. Phys. Condens. Mat. **29**, 305701 (2017).

[13] H. W. Luan, X. Zhang, H. Y. Ding, F. Zhang, J. H. Luan, Z. B. Jiao, Y. C. Yang, H. T. Bu, R. B. Wang, J. L. Gu, C. L. Shao, Q. Yu, Y. Shao, Q. S. Zeng, N. Chen, C. T. Liu, and K. F. Yao, Nat. Commun. **13**, 2183 (2022).

[14] J. Jing, Z. Lu, J. Shen, T. Wada, H. Kato, and M. Chen, Nat. Commun. **12**, 1 (2021).

[15] C. A. Schuh, T. C. Hufnagel, and U. Ramamurty, Acta. Mater. **55**, 4067 (2007).

[16] P. Luo, P. Wen, H. Bai, B. Ruta, and W. H. Wang, Phys. Rev. Lett. **118**, 225901 (2017).

[17] H. B. Yu, K. Samwer, Y. Wu, and W. H. Wang, Phys. Rev. Lett **109**, 095508 (2012).

[18] H. B. Yu, X. Shen, Z. Wang, L. Gu, W. H. Wang, and H. Y. Bai, Phys. Rev. Lett. **108**, 015504 (2012).

[19] Z. Wang, B. Sun, H. Bai, and W. Wang, Nat. Commun. **5**, 5823 (2014).

[20] Y. Sun, S. X. Peng, Q. Yang, F. Zhang, M. H. Yang, C. Z. Wang, K. M. Ho, and H. B. Yu, Phys. Rev. Lett. **123**, 105701 (2019).

[21] G. P. Johari and M. Goldstein, J. Chem. Phys. **53**, 2372 (1970).

[22] P. Guan, M. Chen, and T. Egami, Phys. Rev. Lett. **104**, 205701 (2010).

[23] H. B. Yu, R. Richert, R. Maaß, and K. Samwer, Phys. Rev. Lett. **115**, 135701 (2015).

[24] Y. C. Wu, B. Wang, Y. C. Hu, Z. Lu, Y. Z. Li, B. S. Shang, W. H. Wang, H. Y. Bai, and P. F. Guan, Scripta Mater. **134**, 75 (2017).

[25] Y. J. Duan, J. C. Qiao, T. Wada, H. Kato, Y. J. Wang, E. Pineda, and D. Crespo, Scripta Mater. **194**, 113675 (2021).

[26] J. C. Qiao, Q. Wang, J. M. Pelletier, H. Kato, R. Casalini, D. Crespo, E. Pineda, Y. Yao, and Y. Yang, Prog. Mater Sci. **104**, 250 (2019).

[27] J. C. Qiao, Y. Yao, J. M. Pelletier, and L. M. Keer, Int. J. Plast. **82**, 62 (2016).

[28] L. T. Zhang, Y. J. Duan, T. Wada, H. Kato, J. M. Pelletier, D. Crespo, E. Pineda, and J. C. Qiao, J. Mater. Sci. Technol. **83**, 248 (2021).

[29] T. S. Kê, Scripta. Metall. Mater **24**, 347 (1990).

[30] S. D. Feng, L. Qi, L. M. Wang, P. F. Yu, S. L. Zhang, M. Z. Ma, X. Y. Zhang, Q. Jing, K. L. Ngai, A. L. Greer, G. Li, and R. P. Liu, Scripta Mater. **115**, 57 (2016).

[31] D. Wei, J. Yang, M. Q. Jiang, B. C. Wei, Y. J. Wang, and L. H. Dai, Phys. Rev. B **99**, 014115 (2019).

[32] T. Ichitsubo, E. Matsubara, T. Yamamoto, H. S. Chen, N. Nishiyama, J. Saida, and K. Anazawa, Phys. Rev. Lett. **95**, 245501 (2005).

[33] W. H. Wang, Prog. Mater Sci. **57**, 487 (2012).

[34] X. Bian, G. Wang, Q. Wang, B. Sun, I. Hussain, Q. Zhai, N. Mattern, J. Bednarčík, and J. Eckert, Mater. Res. Lett. **5**, 284 (2017).

[35] J. D. Ferry, *Viscoelastic properties of polymers* (John Wiley & Sons, 1980).

[36] H. Wagner, D. Bedorf, S. Küchemann, M. Schwabe, B. Zhang, W. Arnold, and K. Samwer, Nat. Mater. **10**, 439 (2011).

[37] S. G. Mayr, Phys. Rev. Lett. **97**, 195501 (2006).

[38] Y. J. Duan, D. S. Yang, J. C. Qiao, D. Crespo, J. M. Pelletier, L. Li, K. Gao, and T. Zhang, Intermetallics **124**, 106846 (2020).

[39] B. Shang, J. Rottler, P. Guan, and J. L. Barrat, Phys. Rev. Lett. **122**, 105501 (2019).

[40] E. Pineda, P. Bruna, B. Ruta, M. Gonzalez Silveira, and D. Crespo, Acta. Mater. **61**, 3002 (2013).

[41] G. Williams and D. C. Watts, Trans. Faraday Society **66**, 80 (1970).

[42] J. C. Qiao, Y. J. Wang, L. Z. Zhao, L. H. Dai, D. Crespo, J. M. Pelletier, L. M. Keer, and Y. Yao, Phys. Rev. B **94**, 104203 (2016).

[43] N. Amini, F. Yang, E. Pineda, B. Ruta, M. Sprung, and A. Meyer, Phys. Rev. Mater. **5**, 055601 (2021).

[44] D. Soriano, H. Zhou, S. Hilke, E. Pineda, B. Ruta, and G. Wilde, J. Phys.: Condens. Matter **33**, 164004 (2021).

[45] Y. J. Lü, C. C. Guo, H. S. Huang, J. A. Gao, H. R. Qin, and W. H. Wang, Acta. Mater. **211**, 116873 (2021).

[46] L. M. Wang, R. Liu, and W. H. Wang, J. Chem. Phys. **128**, 164503 (2008).

[47] J. Hachenberg, D. Bedorf, K. Samwer, R. Richert, A. Kahl, M. Demetriou, and W. Johnson, Appl. Phys. Lett. **92** (2008).

[48] F. Zhu, H. K. Nguyen, S. X. Song, D. P. B. Aji, A. Hirata, H. Wang, K. Nakajima, and M. W. Chen, Nat. Commun. **7**, 11516 (2016).

[49] G. P. Johari, J. Chem. Phys. **112**, 7518 (2000).

[50] D. Han, D. Wei, J. Yang, H. L. Li, M. Q. Jiang, Y. J. Wang, L. H. Dai, and A. Zaccone, Phys. Rev. B **101**, 014113 (2020).

[51] M. Goldstein, J. Chem. Phys. **64**, 4767 (1976).

[52] H. L. Smith, C. W. Li, A. Hoff, G. R. Garrett, D. S. Kim, F. C. Yang, M. S. Lucas, T. Swan Wood, J. Y. Y. Lin, M. B. Stone, D. L. Abernathy, M. D. Demetriou, and B. Fultz, Nat. Phys. **13**, 900 (2017).

[53] L. M. Martinez and C. A. Angell, Nature **410**, 663 (2001).

[54] M. H. Tsai and J. W. Yeh, Mater. Res. Lett. **2**, 107 (2014).

[55] Y. Jien Wei, Ann. Chim. Sci. Mat **31**, 633 (2006).